The Plant Cell, Vol. 9, 1481–1493, August 1997 © 1997 American Society of Plant Physiologists

Role of the Proline Knot Motif in Oleosin Endoplasmic Reticulum Topology and Oil Body Targeting

Ben M. Abell,[a] Larry A. Holbrook,[b] Malleva Abenes,[b] Denis J. Murphy,[c] Matthew J. Hills,[c] and Maurice M. Moloney[a,1]

[a]Department of Biological Sciences, University of Calgary, 2500 University Drive Northwest, Calgary, Alberta T2N 1N4, Canada
[b]SemBioSys Genetics Inc., Suite 204, 609 14th Street Northwest, Calgary, Alberta T2N 2A1, Canada
[c]Department of Brassica and Oilseeds Research, John Innes Centre, Norwich Research Park, Norwich NR4 7UH, United Kingdom

An Arabidopsis oleosin was used as a model to study oleosin topology and targeting to oil bodies. Oleosin mRNA was in vitro translated with canine microsomes in a range of truncated forms. This allowed proteinase K mapping of the membrane topology. Oleosin maintains a conformation with a membrane-integrated hydrophobic domain flanked by N- and C-terminal domains located on the outer microsome surface. This is a unique membrane topology on the endoplasmic reticulum (ER). Three universally conserved proline residues within the "proline knot" motif of the oleosin hydrophobic domain were substituted by leucine residues. After in vitro translation, only minor differences in proteinase K protection could be observed. These differences were not apparent in soybean microsomes. No significant difference in incorporation efficiency on the ER was observed between the two oleosin forms. However, as an oleosin–β-glucuronidase translational fusion, the proline knot variant failed to target to oil bodies in both transient embryo expression and in stably transformed seeds. Fractionation of transgenic embryos expressing oleosin–β-glucuronidase fusions showed that the proline knot variant accumulated in the ER to similar levels compared with the native form. Therefore, the proline knot motif is not important for ER integration and the determination of topology but is required for oil body targeting. The loss of the proline knot results in an intrinsic instability in the oleosin polypeptide during trafficking.

INTRODUCTION

The topology of membrane-associated proteins is a critical factor in both their trafficking within cells and their ultimate function. Polypeptides that enter the secretion pathway or that become associated with the endoplasmic reticulum (ER) have been widely studied in yeast and mammals. In most cases in which ER-associated polypeptide topology has been studied, polypeptides with single transmembrane-spanning regions have one terminus in contact with the cytosol and the other terminus exposed to the ER lumen. Proteins such as glycophorin or the low-density lipoprotein receptor have a single membrane-spanning domain with the N terminus positioned luminally and the C terminus in contact with the cytosol. Conversely, the asialoglycoprotein receptor and the transferrin receptor display their N termini in the cytosol and C termini in the ER lumen. Only proteins with multiple membrane-spanning domains appear to retain both N and C termini on the cytosolic side. An example of this is the glucose transport protein of erythrocytes (Wickner and Lodish, 1985; Spiess and Lodish, 1986).

[1]To whom correspondence should be addressed. E-mail mmmolone@acs.ucalgary.ca; fax 403-220-0704.

In plants, there have been relatively few studies of protein topology during intracellular trafficking via the ER. One of the few examples that has received some attention is the tonoplast-integral protein, an aquaporin with structural features derived from the membrane-integral proteins (Reizer et al., 1993), which are an ancient and diverse group of membrane channel proteins. Seed-specific examples of such tonoplast-integral proteins have been reported (Höfte and Chrispeels, 1992). These aquaporins are vacuole localized with six membrane-spanning domains. Both N and C termini protrude on the cytosolic side, whereas loops of ~20 amino acids are exposed on the luminal side. As a group, the plant aquaporins appear to follow existing precedents for proteins with multiple membrane-spanning domains.

The importance of topology is clearly demonstrated by studies on 3-hydroxy-3-methylglutaryl CoA reductase from Arabidopsis. Campos and Boronat (1995) defined the topology by in vitro studies placing the catalytic domain on the cytosolic side of the ER membrane. A switch in topology of 3-hydroxy-3-methylglutaryl CoA would have a critical effect on compartmentalization of its enzyme activity, relocalizing it into the ER lumen.

Oleosins or oil body proteins represent a unique class of ER-processed proteins. These are a family of proteins found associated with oil bodies in seeds (Huang, 1992, 1996; Murphy, 1993) and in some other organs that accumulate oil (Ross and Murphy, 1996). They share a highly conserved hydrophobic domain of ~72 amino acids flanked by two hydrophilic/amphipathic domains of variable length and sequence. The central domain is predicted to reside in the phospholipid monolayer and triacylglycerol (TAG) core of oil bodies, whereas the flanking domains lie against the phospholipid surface (Huang, 1992). Oleosins account for as much as 8% of total seed protein in Brassica seeds.

For oleosins, considerable evidence supports a targeting pathway via the ER (Napier et al., 1996). Qu et al. (1986) demonstrated that the vast majority of oleosin synthesis is directed by membrane-bound polyribosomes in maize. Subsequent studies showed that in vitro–translated oleosin could be targeted to canine pancreatic microsomes but not to erythrocytes, plastids, heat-inactivated canine pancreatic microsomes, or oil bodies (Hills et al., 1993; Loer and Herman, 1993). Although these experiments did not demonstrate the pathway of ER targeting, it has been found that the signal recognition particle is capable of causing translational arrest in vitro (Thoyts et al., 1995). This provides preliminary evidence for a cotranslational, signal recognition particle-mediated targeting pathway but does not rule out post-translational ER targeting of oleosins (Ng et al., 1996). No signal sequence cleavage has been observed during microsome translation (Hills et al., 1993; Loer and Herman, 1993), and a noncleaved signal sequence remains unidentified. In this respect, oleosin is unique, because all other characterized seed storage proteins targeted to the ER are known to possess N-terminal cleavable signal sequences (Chrispeels and Raikhel, 1992). No in vitro study to date has been able to define the topology of the oleosin polypeptide on the ER. Only general observations that some sequences, either the N or C terminus (or both), are exposed to the cytosol (Hills et al., 1993) have been made.

Evidence from electron microscopic studies also suggests that oil bodies are formed from the ER (Wanner et al., 1981). This would colocalize oleosin synthesis and TAG synthesis in the ER (Wanner and Theimer, 1978). However, the intermediate mechanisms of oleosin targeting and association with TAG remain to be determined. A key factor in determining this coordination may be the membrane topology assumed by oleosin. Possible interactions with luminal or cytosolic components will depend on domain orientation. The mechanics of oil body budding will also depend on this conformation.

Theoretical models based on oleosin sequence have suggested a topology in the ER in which the hydrophobic domain is embedded in the phospholipid bilayer and is flanked by two cytosolic domains. If this model is correct, it would be a novel topology among characterized membrane proteins (Wickner and Lodish, 1985). Therefore, a study of its structure and targeting mechanisms is likely to yield important new understanding of ER protein translocation. The small size of oleosins (16 to 24 kD) allows for detailed characterization and may provide insights into the targeting of more complex proteins whose targeting is still not well understood. An example of this is apolipoprotein B, which plays a critical role in lipid transport in mammals (Yao and McLeod, 1994; Innerarity et al., 1996). This could be considered to be an oleosin analog in terms of its ER targeting and role in lipid vesicle stabilization.

The predicted topology of apolipoprotein B bears close resemblance to oleosins in lipoprotein vesicles, although the lipid-associated hydrophobic segments are shorter than the oleosin hydrophobic domain. Association with the ER membrane appears to be transient (Chuck et al., 1990; Nakahara et al., 1994), and association with TAG is mediated by a series of pause transfer sequences that stop and start translocation at defined points (Chuck and Lingappa, 1992). Apolipoprotein B is exposed to the cytosol during translocation, as demonstrated by its sensitivity to trypsin cleavage (McLeod et al., 1996) and degradation by a ubiquitin–proteasome pathway (Yeung et al., 1996). However, the N-terminal 48% of apolipoprotein B is capable of forming very low density lipoproteins and, when translocated into microsomes, is almost completely protected from exogenous trypsin (McLeod et al., 1996), indicating a location in the ER lumen. This inverse topology relative to that proposed for oleosins could account for the direction of particle budding, that is, cytosolic oleosin/TAG particles and secretion of apolipoprotein/TAG particles.

Some studies of oleosin targeting have used oleosin–β-glucuronidase (GUS) translational fusion reporters to assess the importance of individual oleosin domains (Van Rooijen and Moloney, 1995). Oleosin–GUS lacking the central hydrophobic domain accumulated at extremely low levels on oil bodies, whereas the N- and C-terminal domains could be deleted with less severe reductions in oil body accumulation and high targeting efficiencies. This implies the location of a signal sequence in the hydrophobic domain. By investigating oleosin targeting at a finer level and by employing a strategy of site-directed mutagenesis, we are dissecting the targeting pathway to identify critical motifs within oleosin. A key motif for such study is the universally conserved "proline knot" region of the hydrophobic domain (Huang, 1996).

Three prolines distributed over a 12-residue region are present in all known oleosins (Lee et al., 1994). They are predicted to mediate a turn that would facilitate the formation of an antiparallel α helix or β strand (Huang, 1992). By substituting these prolines with other amino acids, a significant structural change is likely to occur. Given the conserved nature of this proline knot, such modifications could reveal its function and help to distinguish between initial ER association and subsequent steps in oleosin targeting. In addition, such modification might change the topology or folding of the protein and specify a different trafficking route. Such a change might help to elucidate the overall mechanism of oleosin targeting. The objectives of this study were to modify the

proline knot and determine the effects on ER association, on oleosin stability, and ultimately, on targeting to oil bodies.

RESULTS

Membrane Topology Determination of Oleosin

To analyze the membrane topology of oleosin, in vitro translation was performed in the presence of canine microsomes. RNA transcribed in vitro from a wild-type oleosin (WTOLEO) cDNA clone was used to program the reaction. The amino acid sequence specified by that cDNA is shown in Figure 1. Membrane incorporation was verified by analyzing pelleted microsomes and also by detecting proteinase K protected fragments. Fragment sizes were determined using a calibration curve generated from a molecular mass marker set ranging from 2.5 to 17 kD (Sigma) and obtained from a single pair of gels. In Figure 2, full-length native WTOLEO can be observed in microsome pellets and yields a protected fragment of an apparent 8.6 kD. The full-length product is predicted to be 18.4 kD but has an apparent size of 17.4 kD. A lower band was also noted. This was assumed to result from either premature chain termination or use of a downstream initiation codon. When the C terminus is deleted (WTOLEO:C^- lacks the C-terminal 56 residues), the protected fragment is smaller (6.8 kD) than that derived from WTOLEO, indicating considerable exposure but partial protection of the C terminus on the external microsome surface near the junction of the hydrophobic and C-terminal domains.

The data support a topology in which hydrophobic domain is embedded in the phospholipid bilayer and is flanked by N- and C-terminal domains located in the cytosol. WTOLEO:N^{-21} lacks the N-terminal 21 amino acids and produced only a single band at the same size as the lower WTOLEO product. This indicates that the initiation of translation at codon 20 or 21 of WTOLEO is responsible for the smaller product. The full N-terminal deletion (WTOLEO:N^- lacks the N-terminal 44 residues) also displays only one band, supporting this conclusion. The N-terminal deletion WTOLEO:N^- has a protected fragment equal in size to that derived from the full-length protein. This clearly demonstrates that the entire N terminus is exposed to protease and must lie on the external surface of the microsomes.

N-terminal domain:

```
MADTARGTHHDIIGRDQYPMMG/RDRDQYQ
1         10         20
MSGRGSDYSKSRQIAK
30        40
```

Hydrophobic domain:

```
AATAVTAGGSLLVLSSLTLVGTVIALTVAT
    50        60        70
PLLVIFSPILVPALITVALLITGFLSSGGF
    80        90        100
GIAAITVFSWIY
    110
```

C-terminal domain:

```
KYATGEHPQGSDKLDSARMKLGSKAQDLKD
  120       130       140
RAQYYGQQHTGGEHDRDRTRGGQHTT
  150       160       170
```

Figure 1. Protein Sequence of Arabidopsis Oleosin.

The sequence is divided to demonstrate truncation points of domain deletions. The slash shows the truncation point in WTOLEO:N^{-21} and PVOLEO:N^{-21}. Underlined proline residues are substituted by leucine residues in PVOLEO and its derivatives.

A Proline Knot Variant of Oleosin Exhibits Alternative Membrane Conformations

The proline knot has been proposed to play a major role in determining the conformation of the hydrophobic domain (Huang, 1992). Therefore, a cDNA variant substituting the three conserved proline codons with leucine codons (PVOLEO for proline knot variant; see Figure 1) was used for in vitro transcription and translation. Leucine residues are common residues in the hydrophobic domain and do not have the rigid peptide linkage imposed by proline residues. The topology of PVOLEO was investigated by generating both truncation and extension constructs. PVOLEO:N^{-21} (N-terminal 21 residue truncation) is similar in size to WTOLEO:N^{-21}, and PVOLEO:N^- (N-terminal deletion) and PVOLEO:C^- (C-terminal deletion) are similar to the WTOLEO:N^- and WTOLEO:C^- truncations, respectively. PVOLEO was also extended at the C terminus by a GUS fusion to yield PVOLEO:GUS.

By integrating the results from these truncations and extensions in WTOLEO and PVOLEO, a proteinase K protection map can be produced. Counterpart proteins in native and proline knot variant forms do not migrate to the same position on the gel, for example, WTOLEO:C^- and PVOLEO:C^- full-length proteins. This is most likely because of structural changes exerted by the proline knot motif, which is amplified in the lower portion of the gel. These discrepancies were taken into account for the deduced model shown in Figure 3, which is consistent with the data and based on the following arguments.

(1) PVOLEO has a full-length band at the same size as WTOLEO, yet the two protected fragments are larger than is the single fragment derived from WTOLEO (10.3 and 11.5 kD). PVOLEO also shows a smaller translation product similar in size to the lower WTOLEO band. PVOLEO:N^{-21} displays a full-length band equal to the lower PVOLEO band, indicating that this lower PVOLEO band also stems from use of a downstream initiation codon at codon 20 or 21. PVOLEO:N^{-21} displays a second lower band that may result from translation

from the initiation codon at position 30 or premature chain termination at a specific site. The size difference would favor the latter explanation.

(2) PVOLEO:N$^-$ displays a single protected fragment at the same size as the lower PVOLEO protected fragment (10.3 kD), which indicates that the larger protected fragment of PVOLEO includes some N terminus. The difference in PVOLEO protected fragments (1.2 kD) corresponds to ~11 residues. The protection of these two fragments implies the existence of two alternative PVOLEO conformations.

(3) The C terminus is mainly exposed but partially protected for WTOLEO and PVOLEO (an apparent 6.8 kD for WTOLEO:C$^-$ and 9.1 and 10.3 kD for PVOLEO:C$^-$) and by similar amounts (a 1.8-kD difference comparing WTOLEO with WTOLEO:C$^-$, and a 1.2-kD difference comparing PVOLEO with PVOLEO:C$^-$). These fragment sizes indicate protection of ~14 residues internal to the C terminus.

(4) The upper PVOLEO:C$^-$ protected band is the same size as the lower PVOLEO protected band (10.3 kD). This indicates that the difference between PVOLEO alternative protected conformations is similar to the protection of the C terminus. Furthermore, this implies that the least protected PVOLEO fragment and the WTOLEO protected fragment have an N terminus close to the N-terminal/hydrophobic domain boundary.

It is also clear from these results that oleosin is capable of efficient membrane incorporation when it is in native or proline knot variant form. It should be noted that the proline knot variant will have increased label incorporation with 19

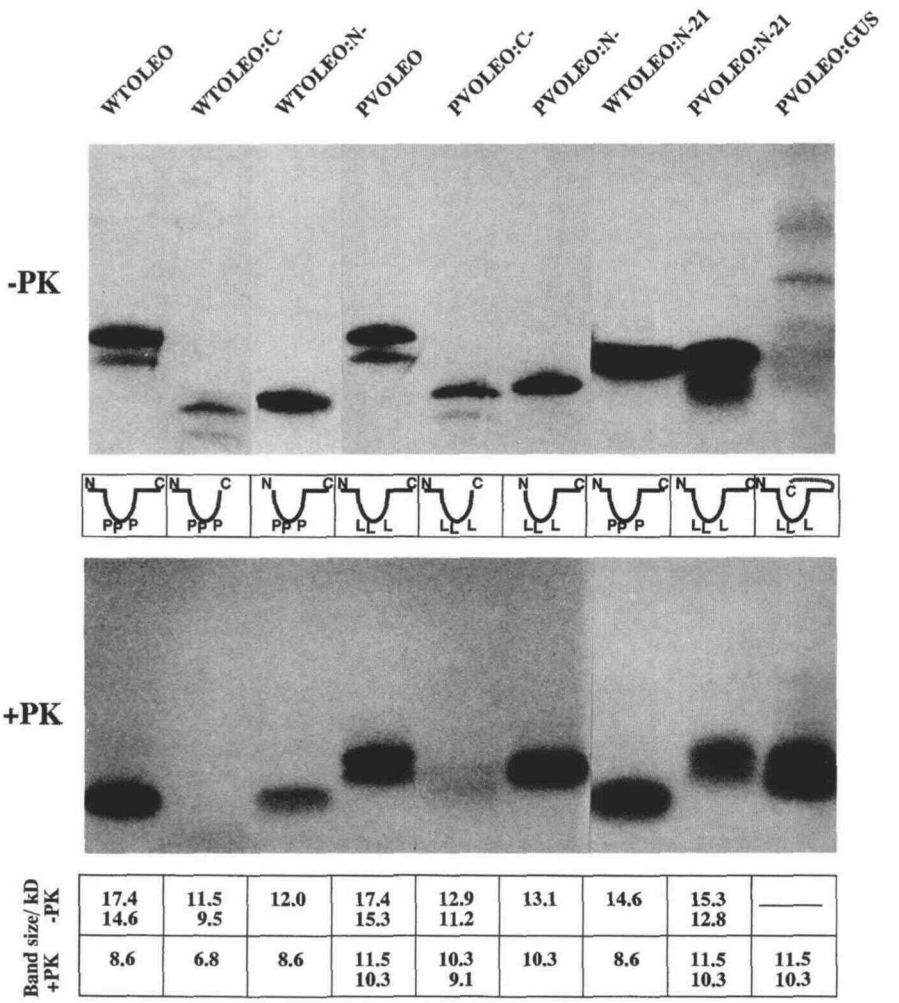

Figure 2. Determination of Oleosin Membrane Topology in the ER.

Oleosin cDNA constructs were in vitro translated using a rabbit reticulocyte lysate with canine pancreatic microsomes and labeled with ^{3}H-leucine. Membrane-incorporated oleosins were pelleted after treatment with (+PK) or without (−PK) proteinase K. Products were separated by SDS-PAGE, using 16% polyacrylamide gels, and monitored by fluorography. N, N terminus; C, C terminus; P, proline residue; L, leucine residue.

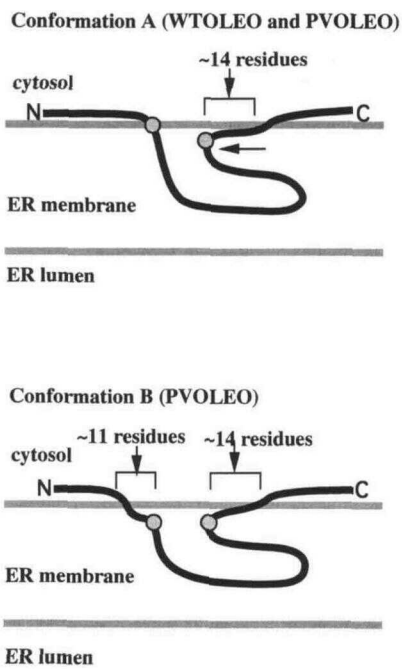

Figure 3. Proteinase K Protection Maps of Oleosin in Native and Variant Forms.

Conformation A represents WTOLEO (native oleosin) and the least protected PVOLEO (proline knot variant) conformations. Conformation B represents the more protected PVOLEO conformation. Shaded circles show the domain boundaries, and the approximate sizes of the protected fragments are given. C, C terminus; N, N terminus.

leucine residues compared with 16 in the native form. Oleosin lacking either the N- or C-terminal domains is capable of stable membrane insertion, although there appears to be some reduction in microsome incorporation for both C-terminal domain deletions. This is partly due to lower label incorporation through the deletion of leucine residues present in the C-terminal domain (three leucine residues deleted). PVOLEO:GUS failed to yield a distinct band at the expected size (86 kD), which is not surprising given the increased probability of premature chain termination, typical of in vitro translation (Ausubel et al., 1995). However, it is clear that a range of extended oleosins are produced and that they generate the same proteinase K protected fragments as PVOLEO. This confirms the location of the C-terminal domain on the outer microsomal surface.

Alternative Proline Knot Variant Conformation Is Stable and Also Observed for Native Oleosin in Soybean Microsomes

To investigate further the alternative PVOLEO protected fragment sizes, the level of proteinase K was increased over a fourfold range. Although Figure 4A shows a loss of total protein typical of excessive protease treatment, the lower band shows only slightly more resistance to proteinase K. This suggests that the two bands represent distinct conformations of oleosin rather than sequential stages of proteolysis.

Soybean microsomes were also prepared from embryos as an alternative to canine microsomes and were treated similarly, as shown in Figure 4B. The sizes of protected fragments were similar to those in canine pancreatic microsomes, but WTOLEO yielded an additional larger protected fragment equivalent to the larger PVOLEO protected fragment. This implies that the alternative conformations are displayed equally by both WTOLEO and PVOLEO in soybean microsomes. These alternative conformations are therefore unlikely to be a critical factor for oil body targeting.

Proline Knot Motif Is Critical in Vivo for Oil Body Targeting of Oleosin–GUS

To investigate the role of the proline knot in oil body targeting in vivo, oleosin–GUS fusion constructs in Agrobacterium were introduced into both *Brassica carinata* and Arabidopsis. A proline knot variant (PVOLEOGUS) was compared with OBPGUSA (native oleosin–GUS), which had already been transformed into *B. carinata* (S. Chaudhary, D. Parmenter, and M.M. Moloney, unpublished results) and introduced into Arabidopsis.

Corresponding constructs in pBluescript KS+ were used in biolistic bombardment for transient expression studies. Flax embryos at a midcotyledonary stage were used primarily because of their high levels of oleosin–GUS expression; however, the experiments were also conducted contemporaneously

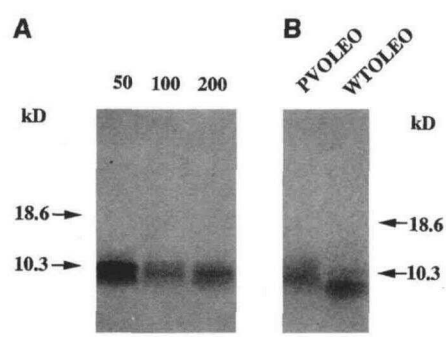

Figure 4. Stability and Specificity of Alternative Oleosin Conformations.

(A) Increasing concentrations of proteinase K (micrograms per milliliter) treatment of in vitro translation product PVOLEO in canine pancreatic microsomes.

(B) Translation of WTOLEO and PVOLEO with soybean microsomes after proteinase K treatment.

Marker sizes indicated at left and right are in kilodaltons.

with both soybean and *B. napus* embryos. Seeds of stable transformants or embryos were homogenized and fractionated into a pellet (discarded) and primary supernatant. This primary supernatant was then further fractionated into the supernatant and oil bodies (floating fat pad). Figure 5 shows the GUS activity that was normalized to protein content in seeds or luciferase activity (introduced by cobombardment) in embryos.

Transgenic *B. carinata* displayed GUS activity 100-fold higher for OBPGUSA relative to PVOLEOGUS (Figure 5A) and an oil body targeting ratio of 61% compared with 18% (Figure 5B), respectively. Similarly, transient expression in flax gave 24-fold higher GUS activity for OBPGUSA compared with PVOLEOGUS (Figure 5C), with a respective oil body targeting of 70% compared with 17% (Figure 5D). GUS activity of wild-type seeds and embryos was significantly lower than for PVOLEOGUS and was too low to measure reliably. The apparently high levels of oil body targeting of this endogenous GUS activity are insignificant when overall accumulation is considered. Similar results were obtained in transgenic Arabidopsis seeds and transient embryo expression in *B. napus* and soybean.

Clearly, substitution of the prolines has a striking effect on both total levels of accumulation of oleosin and oil body targeting efficiency. This effect is essentially the same in both transient expression and stably transformed long-term accumulation. It was possible that the reduced expression levels were due to either reduced transcript levels or the failure of GUS to maintain high activity as a fusion with the proline knot variant. To test the first possibility, gel blotting was performed with RNA from transgenic embryos, and the results are shown in Figure 6.

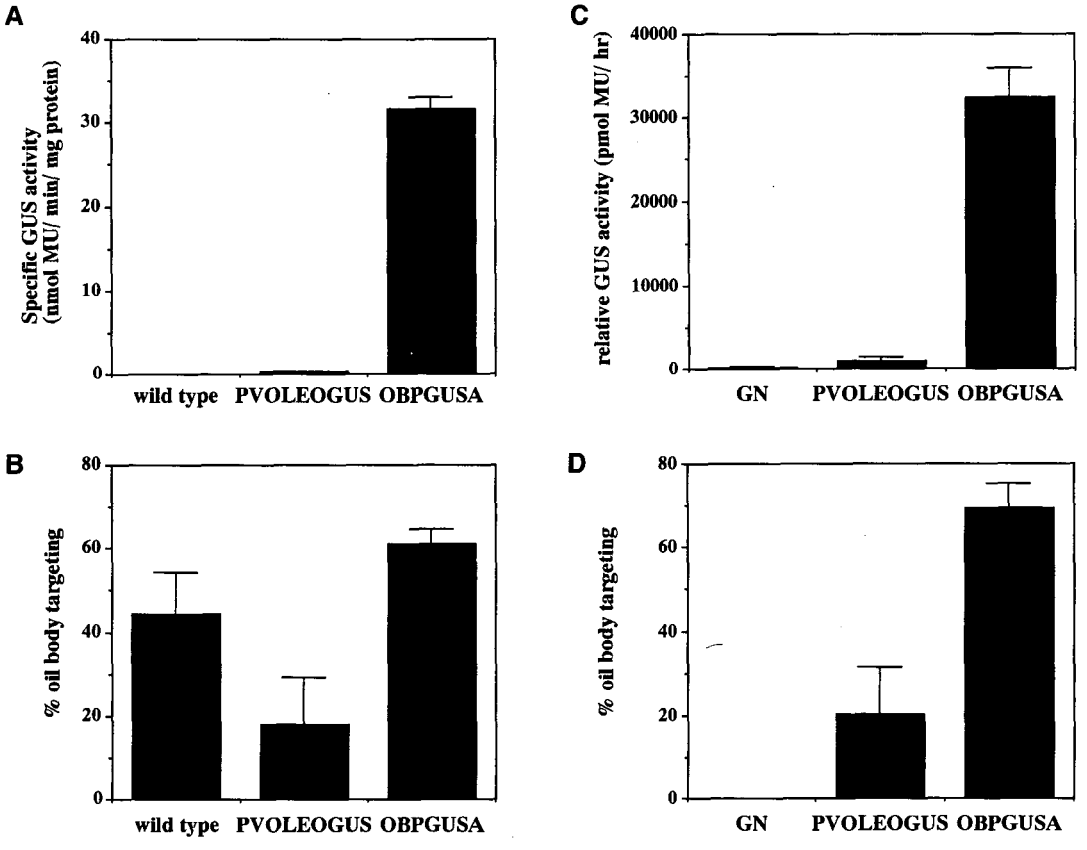

Figure 5. The Proline Knot Variant of Oleosin–GUS Fails to Target Efficiently to Oil Bodies.

(A) GUS activity normalized to protein content in transgenic seeds of *B. carinata*. PVOLEOGUS is the proline knot variant of oleosin–GUS, and OBPGUSA is the native oleosin–GUS.

(B) Oil body targeting corresponding to **(A)**.

(C) GUS activity normalized to luciferase in flax embryo transient expression. GN (pGnos) is a promoterless GUS construct used as a negative control.

(D) Oil body targeting efficiency corresponding to **(C)**.

Error bars represent the standard error of duplicate samples of seeds or triplicate samples of 10 cotyledons. MU, 4-methylumbelliferone.

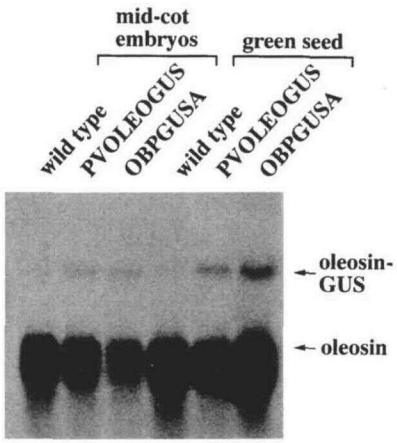

Figure 6. The Oleosin–GUS Transcript Is Expressed at Comparable Levels in OBPGUSA and PVOLEOGUS Plants.

Gel blot analysis of transgenic *B. carinata* midcotyledonary (mid-cot) embryos by using 10 μg of total RNA per lane and an Arabidopsis oleosin cDNA as a probe.

The signal from endogenous oleosin mRNA was used to calculate the relative abundance of oleosin–GUS transcript after scanning the autoradiographs. The PVOLEOGUS transcript was 1.5% of oleosin transcript in midcotyledonary embryos, and the OBPGUSA transcript was a little higher, at 2.8%. Similar values of 1.9 and 2.9%, respectively, were obtained with RNA extracts from late cotyledonary immature zygotic embryos. Therefore, the greatly reduced GUS activity in PVOLEOGUS transformants cannot be accounted for by transcript levels.

To investigate the possible inactivation of GUS in PVOLEOGUS protein, an alternative measure of oleosin–GUS accumulation was performed using immunoblot analysis of total seed protein. In Figure 7, it can be seen that wild-type *B. carinata* produced no detectable signals, whereas *B. napus* GB5 plants (oleosin promoter–GUS; Plant et al., 1994) gave a strong reaction to GUS antibodies at the expected size of free GUS (68 kD). OBPGUSA generated the expected full-length product at 86 kD. PVOLEOGUS failed to generate any detectable full-length oleosin–GUS (expected size, 86 kD). This confirms that the low GUS activity observed in PVOLEOGUS seeds is due to impaired protein accumulation.

Proline Knot Motif Inhibits Association of Oleosin with Oil Bodies and/or Its Stability on Oil Bodies

If oil body targeting of the proline knot variant is unaffected up to and including ER membrane integration, three major processes may be responsible for its poor integration into oil bodies: the proline knot variant may be degraded more rapidly in the ER membrane, oil body incorporation may be prevented, or protein may be rejected or degraded from the oil bodies. To address these possibilities, *B. carinata* midcotyledonary transgenic embryos were analyzed by assaying GUS activity in oil body, microsome, and soluble fractions. Microsomes were isolated by centrifuging the initial supernatant fraction over a 0.5 M sucrose cushion to yield a microsomal pellet and a cleared supernatant. Oil bodies were washed to yield a second supernatant. Recovery of GUS activity ranged from 64 to 96%, except for GB5 embryos, which yielded only 25 and 29%. The lack of efficient recovery was investigated by extending the assays to include the supernatant/sucrose cushion interface and the remaining sucrose cushion. By including these fractions, GUS activity recovery was increased to 78 and 92%. Activity at the supernatant/sucrose cushion interface accounted for 42 and 49% of primary supernatant, and activity at the sucrose cushion accounted for 35 and 42% of primary supernatant.

Consistent with other data presented here, Figure 8 shows that GUS activity in OBPGUSA embryos was mostly located in the oil bodies (mean of 62%), but little GUS activity (mean of 2%) was located in the oil bodies of PVOLEOGUS embryos. However, significant and comparable levels of GUS activity could be detected in the microsome fractions of both OBPGUSA and PVOLEOGUS. This GUS localization is not likely due to nonspecific association because the microsomal activity of nontargeted GUS in GB5 embryos is considerably lower. Clearly, oleosin–GUS in proline variant form accumulates normally or possibly at elevated levels in ER but fails to accumulate subsequently in oil bodies.

The activity detected in the second supernatant of GB5 is due mostly to components in the uncleared supernatant, of which a significant proportion remains in the unwashed oil body fraction (20%) and which can be removed by the

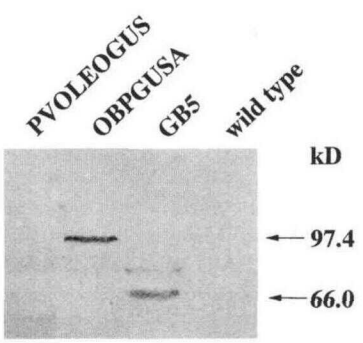

Figure 7. Low GUS Activity of PVOLEOGUS Transformants Is Due to Low Protein Accumulation.

Immunoblot of the GUS polyclonal antibody raised against total seed protein extracts of *B. carinata* and *B. napus* transgenic seeds. PVOLEOGUS is the proline knot variant of oleosin–GUS in *B. carinata*, OBPGUSA is the native oleosin–GUS in *B. carinata*, and GB5 is nontargeted GUS in *B. napus*. Numbers at the right are molecular masses in kilodaltons.

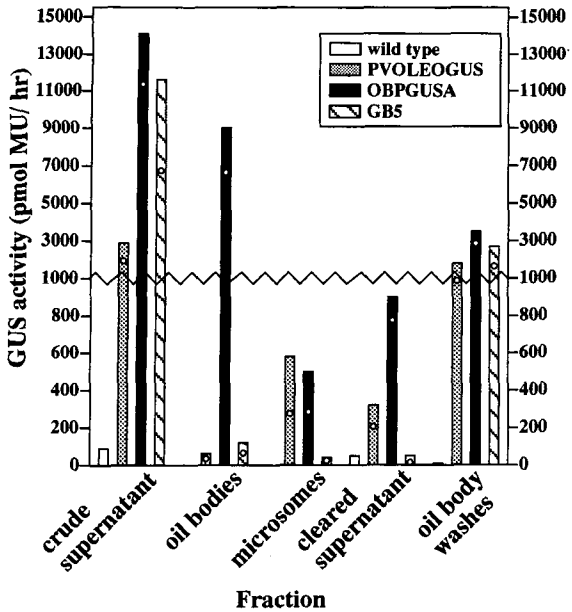

Figure 8. Fractionation of GUS Activity in Transgenic *B. carinata* Midcotyledonary Embryos Expressing Oleosin–GUS.

PVOLEOGUS is the proline knot variant, and OBPGUSA is the native form or free GUS (derived from GB5; transgenic *B. napus*). The cleared homogenate was fractionated into oil bodies, microsomes, and supernatant (cleared by a 93,000*g* spin). White circles represent the repeat values (no repeat for the wild type), and the line at 1000 pmol 4-methylumbelliferone (MU) per hr marks a discontinuity in the graph.

subsequent high-speed centrifugation. However, this is not a sufficient explanation to account for the second supernatant GUS activity in OBPGUSA and PVOLEOGUS embryos. It is possible that some membrane elements containing oleosin–GUS are associated with the fat pad in the initial oil body fraction. These fractions could be released by the detergent (0.1% Triton X-100 and 0.1% sarkosyl) in the second supernatant washes. It is also likely that some oil bodies are lost into these washes.

If the oil body fraction is compared between poorly or nontargeted samples, similar apparent targeting efficiencies can be observed; PVOLEOGUS (2.3%) is similar to endogenous GUS-like activity in the wild type (3.5%) and nontargeted GUS in GB5 (1.1%). This suggests that the observed GUS activity in oil bodies of PVOLEOGUS embryos is purely a nonspecific association.

DISCUSSION

In this study, we dissected the oleosin targeting pathway and identified critical motifs in the protein structure involved in its trafficking. The investigations presented here focus on ER membrane topology and the highly conserved proline knot motif.

Other studies have demonstrated the stable integration of oleosin into microsomal vesicles and an inability to target directly to oil bodies (Hills et al., 1993; Loer and Herman, 1993). These studies, however, were unable to address the question of topology other than to observe that at least one of the termini (N or C) was on the cytoplasmic side. Translation of oleosins has also been demonstrated to be associated with membrane fractions in vivo (Qu et al., 1986). Similarly, however, the membrane topology was not determined in those studies. By creating a series of truncation and extension constructs and using ^{3}H-leucine as the label for in vitro–translated oleosin, we have defined the topology and membrane-protected regions of the native and proline knot variant forms of plant oleosins. Clearly, the flanking amphipathic domains are always exposed on the cytosolic side of the membrane, whereas the hydrophobic domain is membrane protected (Figure 3). The boundaries for membrane protection obtained experimentally are close to those predicted by hydrophobicity plots (Huang, 1996).

Assuming that the hydrophobic domain does not enter the ER lumen because of its extreme hydrophobicity, the determined topology is unique among characterized membrane proteins. Many segments of apolipoproteins may fall into a similar topology type but with luminal rather than cytosolic membrane-associated domains (Yao and McLeod, 1994; Innerarity et al., 1996; McLeod et al., 1996). However, it is clear that for oleosins, the proline knot motif is not critical in directing this topology. The differences in protease protection between native and proline knot variants of oleosins are small and are not even detected when soybean microsomes are used. The inconsistency between microsome preparations may be due to different phospholipid compositions or other factors affecting proteinase K accessibility. It is also possible that the soybean microsomes may have some TAG sequestered in the bilayer and thus present a heterogeneous system. This could affect oleosin conformation. Protection from proteinase K does not correlate precisely with membrane incorporation, and this may explain the partial protection of the C-terminal domain. Charged residues present in this region are highly unlikely to become membrane integrated. A similar situation exists in the N-terminal portion, which gains protection in the alternative proline variant conformation. These sequences may, for example, maintain a tight association with the phospholipid bilayer surface.

The ability of truncated oleosins to be incorporated into membranes was demonstrated previously for a C-terminal deletion in vitro (Thoyts et al., 1995) and in vivo by an oleosin–GUS fusion (Van Rooijen and Moloney, 1995). However, a considerably reduced efficiency of incorporation is observed here, indicating a possible role for the C-terminal domain in translocation. The presence of sequence following the central domain may allow a signal sequence to be fully exposed outside of the ribosome before chain termination. This may facilitate more efficient ER targeting.

It is also not surprising that the N-terminal domain truncation is capable of membrane incorporation. A similar truncation fused to GUS at the C terminus was targeted to oil bodies in transgenic *B. napus* with only a small reduction in accumulation on the oil body (Van Rooijen and Moloney, 1995). These data confirm the fundamental requirement for the hydrophobic domain in ER and oil body targeting.

Oleosin–GUS fusions (native and proline knot variant oleosins) in which GUS includes a glycosylation site are enzymatically active in transgenic plants (data for native form only; Van Rooijen and Moloney, 1995). This is also confirmed by studies using biolistic techniques (data not shown). GUS is inactivated by glycosylation (Iturriaga et al., 1989); therefore, these results imply a cytosolic orientation of GUS and thus the C-terminal domain. These data support the results obtained through the in vitro targeting experiments.

This membrane topology may provide clues relating to the manner in which the insertional process takes place. All other characterized membrane proteins possess opposing orientations of the domains flanking a single membrane-spanning segment (Wickner and Lodish, 1985). The fact that the hydrophobic domain is flanked by two cytosolic domains indicates a stable folding of this domain. This is predicted to be an antiparallel α helix or β strand and to be mediated by the proline knot motif (Huang, 1992). However, the same topology is maintained in association with the proline knot variant. This result was surprising because the loss of this key structural constraint might have led to oleosin polypeptide, assuming a transmembrane topology with N and C termini on opposite sides of the ER. This implies that the proline knot motif is not responsible for insertion into the ER. The proline knot motif may exert more subtle effects on the secondary structure, which is important for downstream targeting events, as discussed below. It is unlikely that this topology is preferred because of interaction with oleosin isoforms (Lee et al., 1995), for although this could occur in the in vivo experiments, no complementary isoforms are present in the canine microsome experiments. The hydrophobic domain must contain a critical feature that supports the cytosolic orientation of both flanking domains. This may involve simply the length of the hydrophobic core.

Recent technical advances have allowed researchers to probe the interactions between translocating polypeptides and the ER membrane (Corsi and Schekman, 1996). Transmembrane domains have been shown to be associated with both a proteinaceous translocation pore and phospholipid components of the membrane in a well-defined sequence (Martoglio et al., 1995; Borel and Simon, 1996; Do et al., 1996). Because the oleosin hydrophobic domain comprises more than twice the size of the number of residues (72) needed for a classical α-helical membrane span, it is likely to impose unique constraints on the translocation process.

Transient expression and stable expression of oleosin–GUS clearly show that the targeting of the proline knot variant to the oil body is greatly impaired. The failure of immunoblotting to detect any full-length oleosin–GUS protein for the proline knot variant in the embryo extracts confirms that the low GUS activity observed is due to poor protein accumulation. The proline knot variant essentially yields the same low expression and inefficient targeting as previously seen with the complete hydrophobic domain deletion (Van Rooijen and Moloney, 1995). This confirms the absolute dependence of proline-induced structure in the hydrophobic domain for accumulation on oil bodies and implies inherent instability of the proline knot variant, presumably because of its inability to accumulate on oil bodies. It is possible that PVOLEOGUS protein fails to target to oil bodies because of the large GUS portion. However, OBPGUSA is highly stable on oil bodies, as demonstrated by its resistance to repeated washes (Figure 8). Any possible effects of the GUS portion are more likely to be an enhancement of the mutation's real effect.

From the fractionation of embryos expressing oleosin–GUS and GUS transgenes, it is clear that oleosin–GUS protein accumulates in the microsomal fraction at a comparable (steady state) level for both PVOLEOGUS and OBPGUSA. This is consistent with the in vitro data, supporting the conclusion that PVOLEOGUS protein is translocated into the ER membrane efficiently. This also suggests that there is no significant change in translation efficiency due to the codon alterations. Because PVOLEOGUS protein accumulates extremely poorly, if at all, in oil body fractions, the deficiency of PVOLEOGUS in targeting is due to either oil body incorporation or its stability on oil bodies. Differences in association of PVOLEOGUS with oil bodies can be accounted for by the different wash procedures used. With the buffer lacking detergents (Figure 8), oil body targeting is apparently 53%, which is reduced to 2% after three washes with the same buffer containing 0.1% Triton X-100 and sarkosyl. An intermediate value of 17% is obtained when the initial homogenization is performed with detergent buffer (Figure 5).

High levels of PVOLEOGUS association with oil bodies can be accounted for by ER contamination of oil bodies. Fractionated *B. napus* embryos contain significantly more ER enzymatic marker in the oil bodies than in the microsomal pellet, as determined by cytochrome *c* reductase (antimycin A–resistant) assays (data not shown). This trapping of ER-derived membrane could account for the PVOLEOGUS found in oil bodies. It also explains the ease by which it is washed away with low concentrations of detergent.

Because the PVOLEOGUS protein is capable of incorporating stably into a phospholipid bilayer, it seems unlikely that it would be intrinsically unstable in oil bodies. In support of this, it is found that additional washes of oil bodies containing PVOLEOGUS, with nondetergent buffer, do not remove GUS activity (data not shown). This is also true when the buffer contains 0.5 M NaCl. In vivo conditions are therefore unlikely to destabilize oil body–incorporated PVOLEOGUS. The low levels of oil body accumulation therefore indicate that it is likely that the proline knot motif is required for oil body packaging. Two distinct possibilities can be suggested to account for such a requirement. One possibility is that the proline knot may introduce a strain into the central

domain or phospholipid bilayer that is relieved upon transition from a phospholipid bilayer to a phospholipid monolayer/TAG core. This thermodynamic drive could provide a bias for oil body incorporation versus ER membrane accumulation. Another possibility is that specific factors depend on the presence of the proline knot motif to coordinate oil body formation.

The nearest comparable mechanisms that might explain this latter possibility can be observed in the coordination of apolipoprotein with TAG to produce lipoprotein vesicles. It has recently been found that apolipoprotein B has a tight physical interaction with the microsomal triglyceride transfer protein (Patel and Grundy, 1996) and is essential for the first step of lipoprotein formation (Gordon et al., 1996). A similar factor(s) might exist in plant embryos to coordinate oil body formation. If these or other factors exist, their interaction may require specific structural motifs in the oleosin. Therefore, further analysis of this variant and others may be useful in understanding the processes and components involved in oleosin/TAG coordination. One reason for instability of the proline knot variant may be its inability to form a heterodimer with an endogenous oleosin isoform. Such a possibility was highlighted by Lee et al. (1995).

In conclusion, oleosins appear to possess a unique membrane topology on the ER. The universally conserved proline knot is not required for ER membrane integration but is an essential feature for subsequent oil body targeting. In the absence of efficient oil body targeting, oleosin is not able to accumulate to high levels in seed cells.

METHODS

Oleosin DNA Constructs

Cloning was performed by standard procedures (Sambrook et al., 1989), and polymerase chain reaction (PCR) was conducted using Pwo polymerase, according to manufacturer's instructions (Boehringer Mannheim). The proline knot substitution was created by PCR-mediated site-directed mutagenesis from the template λ2.1, which contains a genomic oleosin clone from *Arabidopsis thaliana* (Van Rooijen et al., 1992). λ2.1 was used to generate two fragments: GVOP1 by using primers GVR10 (5′-CACTGCAGGAACTCTCTGGTAAGC-3′) and OPK1 (5′-GATAACTAGTAGAAGTGTTGCAACAGTCAAAGCT-3′) with PstI and SpeI sites, respectively; and GVOP2 by using primers OPK2 (5′-CTCTACTAGTTATCTTCAGCCTAATCCTTGTCCTGGCTCTCATCACAGTTGCAC-3′) and GVR01 (5′-AATCCCATGGATCCTCGTGGAACGAGAGTAGTGTGCTGGCCACCACGAGTACGGTCACGGTC-3′) with SpeI and NcoI sites, respectively (the underlined bases comprise the restriction sites used for the cloning).

GVOP1 and GVOP2 were cloned into pBluescript KS+ (Stratagene, La Jolla, CA), and GVOP2 was then subcloned into SpeI and NcoI sites of pGnos (GN; Van Rooijen and Moloney, 1995) to make a translational fusion with β-glucuronidase (GUS) and the nopaline synthase terminator p5.2/1.1. GVOP1 was subcloned into p5.2/1.1 by the common SpeI sites and by ligation of blunted PstI and NotI sites to create pPVOLEOGUS. This mutation was transferred to binary vector by switching common XbaI-XbaI fragments between pPVOLEOGUS and pCGOBPGUSA (Van Rooijen and Moloney, 1995) to create pCGPVOLEOGUS.

cDNA clones for in vitro translation were orientated for T7-driven transcription. pWTOLEO2BP (WTOLEO) was created by PCR from YAP230T7 (obtained from the Arabidopsis Biological Resource Center, Columbus, OH) by using primers Bamoleo (5′-CGCGGATCCATGGCGGATACAGCTAGA-3′) and cAt2a (5′-CCCCCTGCAGTTAAGTAGTGTGCTGGCCAC-3′) with BamHI and PstI restriction sites (underlined), respectively. The PCR fragment was cloned into BamHI and PstI sites of pBluescript KS+. pCPOLEO (PVOLEO) was created by switching common BspEI-AgeI fragments, which include the proline knot coding region. N-terminal deletions of WTOLEO (WTOLEO:N^-) and PVOLEO (PVOLEO:N) were produced by direct cloning of PCR-generated fragments by using primers NTD1 (5′-GCGCGGATCCATGGCTGCAACTGCTGTCACAGC-3′) and cAt2a with BamHI (underlined) and PstI sites, respectively. C-terminal deletions of WTOLEO (WTOLEO:C^-) and PVOLEO (PVOLEO:C^-) were generated similarly by using Bamoleo and CTA1 (5′-CCCCCTGCAGTTAGTAAATCCAAGAGAAAACGG-3′, with PstI site underlined). The N-terminal truncation pCNTB (WTOLEO:N^{-21}) was created from pNTB, a genomic clone lacking the first 21 amino acids of the coding region. pNTB was used as a template for PCR by using primers cAt2b (5′-GCGCGCGGATCCTAAACAAGAACAAAAAAATG-3′) and GVR01 (BamHI site underlined). A BamHI-AgeI fragment was cut from the PCR fragment and used to replace the corresponding fragment in pCNTB. pCBPOL (PVOLEO:N^{-21}) was created by switching the common BspEI-AgeI fragment from pCPOLEO to pWTOLEO2BP. pCPOLEO was extended with *GUS* coding region by switching an ScaI-ScaI fragment from pCPOLEO to pPOLE (pPOLE is a version of pPVOLEOGUS with a glycosylatable GUS).

Transformation of *Brassica carinata*

Cotyledons were transformed using *Agrobacterium tumefaciens* essentially by using the procedure of Moloney et al. (1989). At least five of the highest leaf neomycin phosphotransferase II expressers were chosen for seed GUS assays. The highest GUS expresser was chosen for each construct.

Biolistic Treatments

The DNA was coated onto gold particles by using the protocol of Klein et al. (1988), with minor modifications. Gold particles that were 1.6 μm in diameter (~3 mg) were stored frozen in 50-μL aliquots of water in 500-μL Eppendorf tubes. Upon thawing, 5 to 10 μg of plasmid DNA was added to the tube. This was followed by the addition of 50 μL of 2.5 M $CaCl_2$ and 20 μL of 0.1 M spermidine (free base, tissue culture grade; Sigma). These steps were all preceded by a brief vortexing step and followed by a 5-min incubation on ice. The tubes were vortexed for 4 min at high speed. This preparation was then spun at 10,000 rpm for 15 sec in a microcentrifuge, liquid was carefully decanted, and the particles were resuspended in 250 μL of absolute ethanol (HPLC grade; Fisher, Unionville, Ontario, Canada) by using a pipette. After vortexing, the preparation was respun at 10,000 rpm for 15 sec and decanted, and the particles were resuspended in 60 μL of absolute ethanol (Kartha et al., 1989). After a brief vortexing step, an aliquot of 15 to 18 μL of the gold particles was pipetted onto the center of a sterilized macrocarrier disc. This was al-

lowed to dry in a sterile environment before being used to bombard embryos.

Ten milliliters of sterile 1% agarose was poured into 60-mm Petri plates, solidified, and overlaid with a sterile filter paper disc (Whatman No. 1, 4.5 cm). Ten flax midcotyledonary embryos were laid side by side in random orientation on this disc, filling a 2-cm-diameter circle at the center of the plate. Biolistic treatments were conducted using the PDS-1000/Helium particle gun (Bio-Rad). The conditions are as follows. The microcarrier consisted of 1.6-μm of gold particles (Bio-Rad). The rupture disc was rated for 900 psi. The target was 11 cm from the rupture disc assembly. The chamber vacuum was maintained at 685 mm of mercury. Fifteen to 18 μm of gold/DNA suspension was loaded on the macrocarrier. This gave a DNA delivery of 2.5 μg per shot.

After delivery, the embryos were transferred along with the filter paper to a new Petri plate (6 cm in diameter) containing a standard mixture of 1 to 4 mL (depending on the size of embryos) of NLN medium (Lichter, 1982), with 10 μM racemic abscisic acid (Sigma). They were kept at room temperature in the dark for 24 hr before histochemical staining. Embryos used in targeting experiments were left in the dark at room temperature for 3 days before processing.

Oil Body Targeting Determination

Embryos or seeds were fractionated using the flotation centrifugation method as described by Van Rooijen and Moloney (1995) to generate a crude pellet, oil body fat pad, and supernatant. The oil body fraction was washed to remove remaining soluble fusion protein. Reporter lysis buffer (Promega) was used for embryos for which luciferase assays were required, and GUS extraction buffer (Jefferson, 1987) was used for the transgenic seeds. Targeting efficiency was determined by subtracting first supernatant activity from the unfractionated oil body first supernatant suspension and expressing this effective oil body expression as a percentage of the unfractionated oil body–first supernatant suspension. Localization of GUS activity in the oil body fraction was confirmed by assaying this fraction at least once for each construct.

GUS Assays

Fractions were assayed for GUS activity by the methods described by Jefferson (1987). Samples were incubated with 4-methyl umbelliferone glucuronidase and were sampled at three time points. Sodium carbonate (0.2 M) was used to stop the reaction. The hydrolysis product 4-methyl umbelliferone (MU) was measured by fluorometry on a fluorescence spectrophotometer (model F-2000; Hitachi, Tokyo, Japan; excitation at 365 nm; emission at 455 nm).

RNA Gel Blotting

RNA was extracted from 20 midcotyledonary embryos or 20 green seeds, according to the method of Verwoerd et al. (1989). Ten-microgram samples were electrophoresed, blotted onto a Hybond N+ membrane, probed, and washed according to the manufacturer's (Amersham) instructions, with two additional high-stringency washes (50 mL 0.1 × SSPE [1 × SSPE is 0.15 M NaCl, 10 mM sodium phosphate, 1 mM EDTA, pH 7.4], 0.1% SDS at 65°C for 15 min). The Arabidopsis oleosin cDNA probe was generated from the BamHI-PstI fragment of pWTOLEO2BP by using a random oligonucleotide priming method. The membrane was used to expose x-ray film (Kodak XAR) for 8 and 95 hr to measure both native oleosin and the oleosin–GUS signal within the linear range of the film. The films were scanned using a Macintosh (Cupertino, CA) DeskScan, and the data were analyzed using National Institutes of Health Image software. The percentage of oleosin–GUS transcripts to oleosin transcripts was calculated using the following formula: oleosin–GUS signal/oleosin signal × 8/95 × 100%.

Immunoblotting

Total seed protein was extracted by homogenization of 10 seeds in 350 μL of buffer (50 mM Na_2HPO_4, pH 7.0, 10 mM β-mercaptoethanol, 10 mM Na_2EDTA), the addition of SDS to a final concentration of 2%, and boiling for 10 min. Debris was discarded after a 5-min spin at 13,000*g*. Protein concentrations were checked by SDS-PAGE and adjusted to achieve equal loadings for the immunoblot. Separation was achieved by SDS-PAGE (on a 7.5% acrylamide gel), according to Laemmli (1970). The fusion proteins were detected using GUS primary antibodies (Clontech, Palo Alto, CA) and goat anti-rabbit secondary antibody linked to alkaline phosphatase, according to Ausubel et al. (1995).

In Vitro Translation

Constructs in pBluescript KS+ were transcribed from the T7 promoter by using a Stratagene RNA transcription kit, according to the manufacturer's instructions. Transcript was then used to program a rabbit reticulocyte translation lysate (Promega); 10-μL reactions contained 0.1 μg of transcript, 30% lysate, 110 mM K^+, 0.9 mM Mg^{2+}, 185 kBq ^3H-leucine at 5.6 TBq $mmol^{-1}$ (Amersham), and other components, as described by the manufacturer. Canine pancreatic microsomes were supplemented at 0.5 equivalents per 10 μL and soybean microsomes at 1.0 equivalents per 10 μL. After incubation at 30°C for 60 min, the reactions were held on ice or treated with proteinase K at 50 μg mL^{-1} (unless otherwise indicated) for canine microsomes or 83 μg mL^{-1} for soybean microsomes for 30 min at 0°C. The protease was inactivated by the addition of 10 mM phenyl methylsulfonyl fluoride. Microsomes were diluted to 100 μL with water and pelleted in an ultracentrifuge (model TL100; Beckman, Mississauga, Ontario, Canada) by using a TLA100.2 rotor at 213,000*g* for 20 min at 4°C. Pellets were resuspended in loading buffer and boiled for 3 min before separation by SDS-PAGE (on a 16% acrylamide gel), according to Schagger and von Jagow (1987). Gels were fixed and visualized by fluorography using Amplify, according to the manufacturer's instructions (Amersham).

Soybean Microsome Preparation

Ten grams of midcotyledonary soybean embryos was ground in liquid nitrogen by using a mortar and pestle. The fine powder was homogenized in 50 mL of buffer A (50 mM triethanolamine–acetic acid (TEA-HOAc), pH 7.5, 50 mM KOAc, pH 7.5, 5 mM $Mg(OAc)_2$, 2 mM DTT, 0.25 M sucrose) by mortar and pestle. The homogenate was spun at 1000*g* for 10 min, then at 10,000*g* for 10 min, and finally at 93,000*g* for 90 min in an SW41 rotor (Beckman). The final pellet was resuspended in 8 mL of buffer B (25 mM TEA-HOAc, pH 7.5, 4 mM DTT, 0.25 M sucrose) by gradual additions, using a glass rod and a 2-mL homogenizer (Potter-Elvehjem; Fisher Scientific). Eight milliliters of buffer C (100 mM TEA-HOAc, pH 7.5, 20 mM EDTA) was

added, and after a 10-min incubation, the resuspended pellet was laid on a sucrose cushion (25 mM TEA-HOAc, pH 7.5, 25 mM KOAc, pH 7.5, 2 mM $Mg[OAc]_2$, 4 mM DTT, 0.5 M sucrose) and spun at 93,000*g* for 90 min. The pellet was then resuspended in 300 μL of buffer E (25 mM TEA-HOAc, pH 7.5, 1 mM DTT, 0.25 M sucrose) and homogenized with a 2-mL Potter-Elvehjem homogenizer. The A_{280} from a 10-μL sample in 1 mL of 1% SDS was used to dilute the microsome preparation to 25 units mL^{-1}. Aliquots were frozen in liquid nitrogen and stored at −70°C. One equivalent was defined as 2 μL of this preparation. Immediately before use, microsomes were treated with 40 units mL^{-1} of S7 nuclease with 2 mM $CaCl_2$ at 20°C for 10 min. Nuclease was inactivated by the addition of 4 mM EGTA, pH 8.3.

Subcellular Fractionation of Embryos

Samples of 10 midcotyledonary *B. carinata* embryos were homogenized in 400 μL of extraction buffer (50 mM Na_2HPO_4, pH 7.0, 10 mM β-mercaptoethanol, 10 mM Na_2EDTA) and 2 mM phenyl methylsulfonyl fluoride in a 2-mL Potter-Elvehjem homogenizer for 1 min. The homogenate was spun at 8200*g* for 10 min at 4°C, and the pellet was discarded. A repeat spin was used to discard a second pellet, and a 100-μL sample was removed from this suspension-unfractionated supernatant. The remaining unfractionated supernatant was spun at 16,000*g* for 10 min at 4°C, and ~200 μL of cleared unternatant was removed with a needle syringe. This unternatant was respun, and 150 μL was then mixed with 50 μL of extraction buffer and loaded onto a 600-μL sucrose cushion (0.5 M sucrose, 0.5 M NaCl, 25 mM Na_2HPO_4, pH 7.0, 5 mM β-mercaptoethanol, 5 mM Na_2EDTA). This was spun in a Beckman TL100 ultracentrifuge in a TLS55 swinging bucket rotor at 174,000*g* for 90 min at 4°C. The top 100 μL was collected as a cleared supernatant fraction (SN−), and the remaining liquid was discarded, except when further GB5 fractionations were conducted. In these cases, the next 200 μL was collected as an interface fraction, and the remaining 500 μL was collected as the sucrose cushion. The microsomal pellet was resuspended in 120 μL of GUS extraction buffer. The oil body fraction (80 μL) was washed three times with 200 μL of GUS extraction buffer (50 mM Na_2HP0_4, pH 7.0, 10 mM β-mercaptoethanol, 10 mM Na_2EDTA, 0.1% Triton X-100, 0.1% sarkosyl), floating the oil bodies by spinning at 16,000*g* for 10 min at 4°C. The 600 μL of washes was pooled (supernatant washes, SN+), and the oil bodies were resuspended in a total of 100 μL of GUS extraction buffer.

ACKNOWLEDGMENTS

We thank Dr. Johnathan Napier (IACR-Long Ashton Research Station, University of Bristol, UK) for sharing the method for plant microsome preparation, Joanna Pinto and Sarita Chaudhary for technical assistance with plant transformation, and Dr. Jean Vance (Lipid and Lipoprotein Research Group, University of Alberta, Edmonton, Canada) for critical reading of the manuscript. We gratefully acknowledge the financial support of the Natural Sciences and Engineering Research Council (Research Grants Program) and the Alberta Agriculture Research Institute.

Received March 5, 1997; accepted May 12, 1997.

REFERENCES

Ausubel, F.M., Brent, R., Kingston, R.E., Moore, D.D., Seidman, J.G., Smith, J.A., and Struhl, K., eds (1995). Current Protocols in Molecular Biology. (New York: John Wiley and Sons).

Borel, A.C., and Simon, S.M. (1996). Biogenesis of polytopic membrane proteins: Membrane segments assemble within translocation channels prior to membrane integration. Cell **85,** 379–389.

Campos, N., and Boronat, A. (1995). Targeting and topology in the membrane of plant 3-hydroxy-3-methylglutaryl coenzyme A reductase. Plant Cell **7,** 2163–2174.

Chrispeels, M.J., and Raikhel, N.V. (1992). Short peptide domains target proteins to plant vacuoles. Cell **68,** 613–616.

Chuck, S.L., and Lingappa, V.R. (1992). Pause transfer: A topogenic sequence in apolipoprotein B mediates stopping and restarting of translocation. Cell **68,** 9–21.

Chuck, S.L., Yao, Z., Blackhart, B.D., McCarthy, B.J., and Lingappa, V.R. (1990). New variation on the translocation of proteins during early biogenesis of apolipoprotein B. Nature **346,** 346–385.

Corsi, A.K., and Schekman, R. (1996). Mechanism of polypeptide translocation into the endoplasmic reticulum. J. Biol. Chem. **271,** 30299–30302.

Do, H., Falcone, D., Lin, J., Andrews, D.W., and Johnson, A.E. (1996). The cotranslational integration of membranes into the phospholipid bilayer is a multistep process. Cell **85,** 369–378.

Gordon, D.A., Jamil, H., Gregg, R.E., Olofsson, S., and Boren, J. (1996). Inhibition of the microsomal triglyceride transfer protein blocks the first step of apolipoprotein B lipoprotein assembly but not the addition of bulk core lipids in the second step. J. Biol. Chem. **271,** 33047–33053.

Hills, M.J., Watson, M.D., and Murphy, D.J. (1993). Targeting of oleosins to the oil bodies of oilseed rape (*Brassica napus* L.). Planta **189,** 24–29.

Höfte, H., and Chrispeels, M.J. (1992). Protein sorting to the vacuolar membrane. Plant Cell **4,** 995–1004.

Huang, A.H.C. (1992). Oil bodies and oleosins in seeds. Annu. Rev. Plant Physiol. Plant Mol. Biol. **43,** 177–200.

Huang, A.H.C. (1996). Oleosins and oil bodies in seeds and other organs. Plant Physiol. **110,** 1055–1061.

Innerarity, T.L., Boré, J., Yamanaka, S., and Olofsson, S.-O. (1996). Biosynthesis of apolipoprotein B48-containing lipoproteins. J. Biol. Chem. **5,** 2353–2356.

Iturriaga, G., Jefferson, R.A., and Bevan, M.W. (1989). Endoplasmic reticulum targeting and glycosylation of hybrid proteins in transgenic tobacco. Plant Cell **1,** 381–390.

Jefferson, R.A. (1987). Assaying chimeric genes in plants: The GUS gene fusion system. Plant Mol. Biol. Rep. **5,** 387–405.

Kartha, K.K., Chibbar, R.N., Georges, F., Leung, N., Caswell, K., Kendall, E., and Qureshi, J. (1989). Transient expression of chloramphenicol acetyl transferase (CAT) gene in barley cell cultures and immature embryos through microprojectile bombardment. Plant Cell Rep. **8,** 429–432.

Klein, T.M., Harper, E.C., Svab, Z., Sanford, J.C., Fromm, M.C., and Maliga, P. (1988). Stable genetic transformation of intact *Nic-*

otiana cells by the particle bombardment process. Proc. Natl. Acad. Sci. USA **85,** 8502–8505.

Knott, T.J., Pease, R.J., Powell, L.M., Wallis, S.C., Rall, S.C., Jr., Innerarity, T.L., Blackhart, B., Taylor, W.H., Marcel, Y., Milne, R., Johnson, D., Fuller, M., Lusis, A.J., McCarthy, B.J., Mahley, R.W., Levy-Wilson, B., and Scott, J. (1986). Complete protein sequence and identification of structural domains of human apolipoprotein B. Nature **323,** 734–742.

Laemmli, U.K. (1970). Cleavage of structural proteins during the assembly of the head of bacteriophage T4. Nature **227,** 680–685.

Lee, K., Bih, F.-Y., Learn, G., Ting, J.T.L., Selles, C., and Huang, A.H.C. (1994). Oleosins in the gametophytes of *Pinus* and *Brassica* and their phylogenetic relationship with those of various species. Planta **193,** 461–469.

Lee, K., Ratnayake, C., and Huang, A.H.C. (1995). Genetic dissection of the co-expression of genes encoding the two isoforms of oleosins in the oil bodies of maize kernel. Plant J. **7,** 603–611.

Lichter, R. (1982). Induction of haploid plants isolated from pollen of *Brassica napus.* Z. Pflanzenzuecht. **105,** 427–434.

Loer, D., and Herman, E. (1993). Cotranslational integration of soybean (*Glycine max*) oil body membrane protein oleosin into microsomal membranes. Plant Physiol. **101,** 993–998.

Martoglio, B., Hofmann, M.W., Brunner, J., and Dobberstein, B. (1995). The protein-conducting channel in the membrane of the endoplasmic reticulum is open laterally toward the lipid bilayer. Cell **81,** 207–214.

McLeod, R.S., Wang, Y., Wang, S., Rusinol, A., and Links, P. (1996). Apolipoprotein B sequence requirements for hepatic very low density lipoprotein assembly. J. Biol. Chem. **271,** 18445–18455.

Moloney, M.M., Walker, J.M., and Sharma, K. (1989). High efficiency transformation of *Brassica napus* using *Agrobacterium* vectors. Plant Cell Rep. **8,** 238–242.

Murphy, D.J. (1993). Structure, function and biogenesis of storage lipid bodies and oleosins in plants. Prog. Lipid Res. **32,** 247–280.

Nakahara, D.H., Lingappa, V.R., and Chuck, S.L. (1994). Translocational pausing is a common step in the biogenesis of unconventional integral membrane and secretory proteins. J. Biol. Chem. **269,** 7617–7622.

Napier, J.A., Stobart, A.K., and Shewry, P.R. (1996). The structure and biogenesis of plant oil bodies: The role of the ER membrane and the oleosin class of proteins. Plant Mol. Biol. **31,** 945–956.

Ng, D.T.W., Brown, J.D., and Walter, P. (1996). Signal sequences specify the targeting route to the endoplasmic reticulum. J. Cell Biol. **134,** 269–278.

Patel, S.R., and Grundy, S.M. (1996). Interactions between microsomal triglyceride transfer protein and apolipoprotein B within the endoplasmic reticulum in a heterologous expression system. J. Biol. Chem. **271,** 18686–18694.

Plant, A.L., Van Rooijen, G.J.H., Anderson, C.P., and Moloney, M.M. (1994). Regulation of an *Arabidopsis* oleosin gene promoter in transgenic *Brassica napus*. Plant Mol. Biol. **25,** 193–205.

Qu, R., Wang, S., Lin, Y., Vance, V.B., and Huang, A.H.C. (1986). Characteristics and biosynthesis of membrane proteins of lipid bodies in the scutella of maize (*Zea mays* L.). Biochem. J. **235,** 57–65.

Reizer, J., Reizer, A., and Saier, M.H. (1993). The MIP family of integral membrane channel proteins: Sequence comparisons, evolutionary relationships, reconstructed pathway of evolution, and proposed functional differentiation of the two repeated halves of the proteins. Crit. Rev. Biochem. Mol. Biol. **28,** 235–257.

Ross, J.H.E., and Murphy, D.J. (1996). Characterization of anther-expressed genes encoding a major class of extracellular oleosin-like proteins in the pollen coat of Brassicaceae. Plant J. **9,** 625–657.

Sambrook, J., Fritsch, E.F., and Maniatis, T. (1989). Molecular Cloning: A Laboratory Manual. (Cold Spring Harbor, NY: Cold Spring Harbor Laboratory Press).

Schagger, H., and von Jagow, G. (1987). Tricine–sodium dodecyl sulfate–polyacrylamide gel electrophoresis for the separation of proteins in the range from 1 to 100 kD. Anal. Biochem. **166,** 368–379.

Spiess, M., and Lodish, H.F. (1986). An internal signal sequence: The asialoglycoprotein receptor membrane anchor. Cell **44,** 177–185.

Thoyts, P.J.E., Millichip, M.I., Stobart, A.K., Griffiths, W.T., Shewry, P.R., and Napier, J.A. (1995). Expression and in vitro targeting of a sunflower oleosin. Plant Mol. Biol. **29,** 403–410.

Van Rooijen, G.J.H., and Moloney, M.M. (1995). Structural requirements of oleosin domains for subcellular targeting to the oil body. Plant Physiol. **109,** 1353–1361.

Van Rooijen, G.J.H., Terning, L.I., and Moloney, M.M. (1992). Nucleotide sequence of an *Arabidopsis thaliana* oleosin gene. Plant Mol. Biol. **18,** 1177–1179.

Verwoerd, T.C., Dekker, B.M.M., and Hoekma, A. (1989). A small-scale procedure for the rapid isolation of plant RNAs. Nucleic Acids Res. **17,** 2362.

Wanner, G., and Theimer, R.R. (1978). Membranous appendices of spherosomes (oleosomes). Planta **140,** 163–169.

Wanner, G., Formanek, H., and Theimer, R.R. (1981). The ontogeny of lipid bodies (spherosomes) in plant cells. Planta **151,** 109–123.

Wickner, W.T., and Lodish, H.F. (1985). Multiple mechanisms of protein insertion into and across membranes. Science **230,** 400–407.

Yang, C.-Y., Chen, S.-H., Gianturco, S.H., Bradley, W.A., Sparrow, J.T., Tanimura, M., Li, W.-H., Sparrow, D.A., DeLoof, H., Rosseneu, M., Lee, F.-S., Gu, Z.-W., Gotto, A.M., and Chan, L. (1986). Sequence, structure, receptor-binding domains and internal repeats of human apolipoprotein B-100. Nature **323,** 738–742.

Yao, Z., and McLeod, R.S. (1994). Synthesis and secretion of hepatic apolipoprotein B–containing lipoproteins. Biochim. Biophys. Acta **1212,** 152–166.

Yeung, S.J., Chen, S.H., and Chan, L. (1996). Ubiquitin-proteasome pathway mediates intracellular degradation of apolipoprotein B. Biochemistry **35,** 13843–13848.